Original Article

Lung CT image Segmentation Using Pix2Pix Model

Vanita D. Jadhav[1], Dr. Lalit V. Patil[2]
[1]PhD Research Scholar, SKNCOE, Vadgaon, Pune, India
[2]Professor, SKNCOE, Vadgaon, Pune, India
DOI: 10.47750/pnr.2022.13.S09.295

Abstract

An important first phase in the computerized diagnosis of the lung computed tomography(CT) scan images is automatic lung segmentation. However, current techniques do not precisely segment the lung in the presence of dense irregularities. This research proposes an improved lung segmentation accuracy approach based on generative adversarial networks (GANs).Effective segmentation of the lung area from the nearby chest area is achieved by proposed network. In order to achieve image segmentation, we used Pix2Pix model and took usage of their ability to convert images. With the use of generative adversarial networks, the unique lung CT image was transformed into the segmented image. Investigational study makes use of the ILD dataset that is openly accessible. The experimental study demonstrates that the projected Pix2Pix model performance is unaffected by the existence of compact irregularities in lung CT.

Keywords: Deep learning; Lung Segmentation; Lung cancer;lung segmentation map; lung CT image; pulmonary nodule.

1. INTRODUCTION

Lung malignancy is the maincauses of death. American Cancer Society's most recent statistics show that there are an estimated 228,000 novel cases of lung cancer, 135,000 of which result in death[58].According to study, lung cancer is treatable in a small percentage of cases that are discovered at an initial stage, whilebulk of the time, a delayed diagnosis and subsequent treatment results in death [1, 2].Therefore, to raise the patient's chances of existence, early detection of lung cancer is essential. CT scanning is the preferred method for diagnosing lung diseases. Even for experienced radiologists, manual lung disease detection and marking requires a lot of time and effort because modern CT scanners generate a lot of CT scans. An automatic Computerized Diagnosis of lung CT scan with a goal of assisting the Radiologists is an efficient remedy for this. The effectiveness of the lung segmentation procedure determines the effectiveness of the entire Computerized Analysis system for detecting lung disease.

Due to the multimodality, grey level fuzziness, and unpredictability of lung images, many segmentation algorithms perform poorly on them. Particularly modest in size are pulmonary nodules. Even some nodules are concealed. After the segmentation information has not been correctly processed, these nodules are challenging for standard deep learning models to detect. This research presented a segmentation technique based on GAN to address this issue. To adopt lung images, we used the Pix2Pix networks, a type of GAN.A blurred image can be translated into an exact image using the Pix2Pix image translation method. We used Pix2Pix to convert lung CT picture to the segmented one. The segmented picture was taken as an accurate image, and the unique lung image was taken as a blurry image. The blurred image was then converted into an exact image using Pix2Pix. Translation's output served as the segmentation outcome. On a data set of lung imaging, the Pix2Pix segmentation approach was tested. Experimental findings show that this research is efficient and performs well than existing advanced techniques. The following Section discusses the similar lung segmentation techniques currently in use.

Because of the obvious change in attenuation in a typical Lung CT image, its straightforward to distinguish among the non-lung and lung region[7].Thus, early methods used approach based on Grey-level thresholding for lung segmentation [10–15].Sun et al. used a region-growing technique built on grey value, gradient magnitude, and region homogeneity to segment the lung area[12]. On normal lung CT scans without abnormal lung tissue patterns, these traditional techniques work effectively. When ILD patterns like fibrosis, lung nodules, ground glass, etc. are present, the conventional thresholding-based techniques do not segment the lung in these areas.

To reduce lung segmentation error, approaches developed in the existing literature [16–21] are created to contain the irregular lung tissue forms. An adaptive boarder marching procedure which walks alongside the boarder of segmented lung and corrects it for identifying the Lung's inner boarder is presented by Pu et al. [7].The technique was developed specifically to segment the lungs while taking into account the juxtapleural nodules.Ye et al. [22] suggested shape-based strategy for the incorporation of segmentation of the lungs' irregular patterns. They suggested the contour correction method based on chain code, wherein important serious spots and lung boundary were found, and then these critical points were joined to obtain an exact lung boundary. However, this approach could result in excessive segmentation when including greater abnormal lung structure. Additionally, Choi et al. linked only those essential sites whose slope is lower than the predetermined threshold by taking slope information from the lung boarder's chain code into consideration[23].Recently, Shen et al. suggested a technique based on support vector machine (SVM) classifier and enhanced bi-directional chain coding mechanism for nodule inclusion[24]. Performance of system depends on the classifier, adaptive threshold and scan quality because of theprocess's cascading nature. Zhou et al. projected amulti-stage technique for inclusion of juxtapleural nodule [20].For lung segmentation, a level set-based methodis suggested by authors in [25, 26]. Furthermore, for lung segmentation,a hybrid geometric active contour method has been developed by Zhang et al. [27]. Active contour modelling is used by Filho et al. for lung segmentation [28]. These techniques, however, require prior shape knowledge. For automatic lung segmentation, numerous intensity-based techniques have been put forth in the body of existing literature [29–42]. The effectiveness of intensity-based lung segmentation methods heavily relies on the ability to extract robust features. A non-negative matrix factorization technique tailed by the traditional k-means clustering techniqueis used by Hosseini-Asl et al. to obtain the necessary features for lung segmentation [29].Furthermore, by adding incremental constraints to it, authors of [30] enhanced the NMF-based technique for three-dimensional lung segmentation. Factorizing the input data, which aid in feature selection, is the key principle underlying NMF's success in segmentation [43].Methods [29,30] that successfully use juxta pleural nodules and pulmonary vessels fail when there are severe irregular lung tissue forms. The NMF algorithm's unsupervised nature prevents it from detecting the abnormal lung tissue pattern, which is why it fails.

Researchers have investigated the CNNs robustness for applications like computer vision since the previous decade [44–53]. Several methods-based on CNN for medical image analysis has been proposed together with natural image processing. Small convolutional filters have been shown to be advantageous for image recognition tasks by Simonyan et al. [48]. In general, selecting the right filter size is a key component of deep network construction. The ideal mix of filter sizes cannot be determined by any general criterion. Szegedy et al. proposed the inception module, a parallel convolution filter bank, as a remedy for this problem [49]. By allowing the network to choose its own optimal route, the Inception module aids in overcoming the challenges of network design. Huang et al. suggested DenseNet based on Deep networks. They used the feature map reuse concept, which is easy to train and results in condensed models [50].In order to improve deep networks regardless of the different network parameters and network depth, He et al. projected the residual learning approach (ResNet) [51]. To solve the vanishing gradient problem, He developed the knowledge of identity mappings. Method based on Deep Deconvolutional Residual Network (DDRN) for lung segmentation is introduced by Singadkar et al.[53]. The method was based on completely training the network before extracting the wide range of nodules from the 2D set of CT images. Convolution neural networks were tested for their suitability for analyzing lung CT scans by researchers [31–41]. For segmenting lung pathologies, a multi-path deep network was presented by Harrison et al. [37]. They made use of the deep network's capacity to learn various ILD tissue pattern types. Additionally, [39] proposes a small CNN model to divide the retrieved part into lung and non-lung regions. The approach's performance is limited to the local area only since it is patch-level, and it is not able to extract the lung region's coarse-level features, which are necessary for including the severely abnormal lung tissue patterns. A volumetric segmentation network (VNet) was proposed by Negahdar et al. for lung segmentation [40]. The multi-view CNN, central pooling approach, improved U-Net, and residual UNet are a few other methods for including abnormal lung tissue patterns, specifically lung nodules [31-34].Despite the fact that performance of the current lung segmentation algorithms has been steadily improving, there is still potential to suggest a generic lung segmentation approach that can take into consideration various ILD pattern types. As was previously said, the segmentation approach is impacted by the different shape, size, and textural aspects of the distinct ILD patterns. Therefore, for lung segmentation, a strong learning technique that could adjust to the presence change of dissimilar ILD patterns is required. For the image-to-image style transfer problem, Isola et al. recently suggested a solution based on c-GAN [55]. The generative models' strong learning capabilities were used by them to predict the missing textural characteristics in an image. Additionally, a C-GAN-based method for segmenting brain tumours was suggested by Nema et al. [52].

2. Methods

2.1 Generative Adversarial Network (GAN)

GAN uses an algorithm that continuously plays competitive games to reach the optimization goal. It is made up of a discriminator and a generator. The generator's primary goal is to produce enough misleading images to prevent the discriminator from determining whether or not they are true. The discriminator's job is to protect them from the generator's deception. The classical generative models typically need for parameter estimation, which calls for intricate calculations like Monte Carlo sampling. GAN doesn't need complex probability calculations, in contrast to conventional generative models. The distribution type is not required to specify in GAN. The distribution is straight replicated by means of deep neural networks and real data. BP method based gradient descent algorithm is typically used during training step. The following can be written as the GAN's optimization function:

$$\min_G \max_D V(D,G) = E_{x\sim p_{data}(x)} \log D(x) + E_{z\sim p_z(z)} \log(1 - D(G(z))) \quad \text{(eq.1)}$$

where D is discriminator,

G is generator,

x is real image,

z is noise input of the generator G,

G (z) isimage generated by generator G,

D (x) is probability that the discriminator D courts

whether the real image istrue, and

D (G (z)) is probability that the discriminator courts

whether the image generated by the generator G

is trueornot.

The goal of Generative Adversarial Network is to discover the training data dissemination. First, a noise is lead into the generator to achieve this purpose. The generator turns this noise into a visual representation. These simulated images are famed from the real image by the discriminator. The generator and the discriminator are both enhanced by cyclic alternate training. The generator is capable of producing artificial visuals that closely resemble the genuine images.

2.2 Pix2Pix

A framework called Pix2Pix was created using conditional Generative Adversarial Network (cGAN). Pix2Pix has a generator (G) and a discriminator (D) in a similar way. One image appears as both G's input and output. To certify that the output image matches the input image, conditional GAN's loss function has the following form.

$$\Gamma_{cGAN}(G,D) = E_{x,y}\left[\log D(x,y)\right] + E_{x,z}\left[\log(1 - D(x, G(x,z)))\right] \quad \text{(eq.2)}$$

where G is generator,

D is discriminator,

z is input random vector,

x is image to be converted

y is target image.

Γ_{cGAN} is conditional GAN loss function.

A lot of info is transmitted between generator G's input and output throughout the image translation process. A L1 loss is introduced to certify that the input image and the output image are highly similar.

$$\Gamma_{L1}(G) = E_{x,y,z}\left[\left\|y - G(x,z)\right\|_1\right] \quad \text{(eq.3)}$$

Finally, the conditional GAN loss function and a L1 loss function are combined to create the Pix2Pix loss function. Solution of Pix2Pix is written as follows :-

$$G^* = \arg\min_G \max_D \Gamma_{cGAN}(G,D) + \lambda\Gamma_{L1}(G) \quad \text{(eq.4)}$$

Where ,

$\Gamma_{cGAN}(G,D)$ is the conditional GAN Loss fuction,

$\Gamma_{L1}(G)$ is added L1 Loss fuction, and G* is final result.

2.3 Lung CT image segmentation by Pix2Pix

A model called Pix2Pix can convert a blurry image into a precise image. To convert the original lung CT image to the segmented lung CT image, we used Pix2Pix. We created the segmented image as an exact representation of the original gray scale lung CT image. The blurred image was then converted into an exact image using Pix2Pix. Translation's output served as the result of segmentation.

3. RESULTS

3.1 Experimental environments

Our research was based on a high-level neural networks API,Keras, developed in Python 3.8 that can be used on top of Tensor flow and operates without a hitch on both the CPU and GPU. The suggested network is trained on a computer with an Intel Core i7 processor clocked at 4.20 GHz and an NVIDIA GTX 1080 8 GB GPU to precisely segment the lung field. As a result, we run our code on a GPU with a Tensor flow backend to significantly speed up execution.

3.2 Data set

This study uses anInterstitial Lung Disease (ILD) dataset [5] to provide the labeled data needed to refine the planned Networks ability to segment the lung accurately. Depeursing et al. [5] created the ILD database to offer a standard platform for assessing automated ILD analysis methods. In the database, 108 high-resolution lung CT (HRCT) scans with annotated lung field maps are available. Each lung CT scan has 20 lung CT slices on average. One of the interstitial lung disorders identified by these scans includes lung tissue patterns such as consolidation, reticulation, fibrosis, lung nodules, ground glass, emphysema, etc.The training dataset is created using 67 out of 108 HRCT scans from the ILD dataset. While the suggested model for lung segmentation is validated using the remaining lung CT scans. Additionally, a data augmentation strategy is used to expand the training dataset by taking into account the flipping technique and picture transpose operators. To train the proposed model for

precise lung segmentation, 6000 lung CT slices with any type of interstitial lung disease are constructed, along with their accompanying lung field segmentation maps. Samples of training images along with their related ground truths are displayed in fig.1. Samples of test images along with their related ground truths are displayed in fig.2.

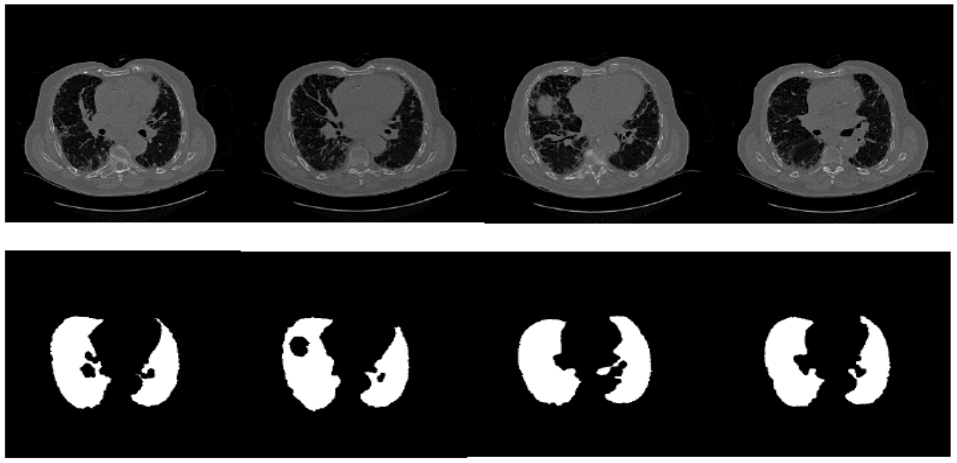

Fig. 1. Samples of training images along with their related ground truths.

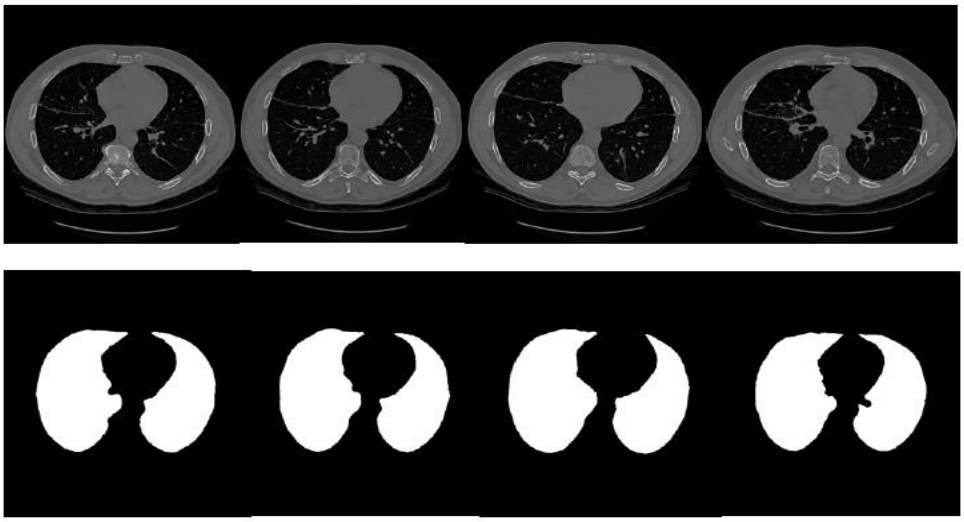

Fig. 2. Samples of test images along with their related ground truths

3.3 Performance evaluation

Test images that were manually segmented by specialists were related to the segmentation results of ground truth images. The F measure, overlap rate, and accuracy were computed. The following are the computation formulas:

$$Accuracy = (TP + FN) / (TP + TN + FP + FN) \quad \text{(eq.5)}$$

$$Overlap\ rate = |A \wedge B| / |A \vee B| \quad \text{(eq.6)}$$

$$F = 2P * R / (P + R) \quad \text{(eq.7)}$$

Where,

TP - true positive rate,

FP - false positive rate,

TN - true negative rate,

FN - falsenegativerate.

A -Segmentation result of Pix2Pix,

B -Image segmented manually by experts,

P - Precision,

R -Recall, and

F - F measure.

3.4 Experimental outcomes

The investigational results of lung segmentation using Pix2Pix are displayed in Table 1. 130 training loops were used. Table 1 show that the average lung segmentation accuracy using Pix2Pix is 93.42%. The accuracy has a range of [56.14%, 96.01%] with a standard deviation of 7.07%. The average overlap of the lung segmentation based on Pix2Pix is 91.70%. The overlap has a range of [32.68%, 97.55%], and its standard deviation is 13.03%. Pix2Pix-based lung segmentation had an average F measure of 95.03%. The F measure has a range of [49.26%, 98.75%] and a standard deviation of 9.67%. Figure 3 displays a few test image examples together with the associated experimental findings. Figure 3 shows that Pix2Pix's segmentation results come close to being faithful to the original image. Experimental findings show that our suggested strategy is efficient and produced notable performance.

Table 1. Investigation a lout comes of Pix2Pix method

	Min	Max	Mean	Standard Deviation
Accuracy	0.5614	0.9601	0.9342	0.0707
Overlap Rate	0.3268	0.9755	0.9169	0.1303
F Measure	0.4926	0.9875	0.9503	0.0967

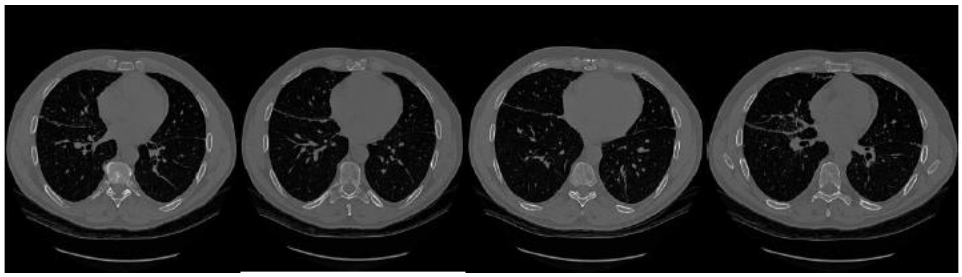

(a) Test Lung CT images

(b) Ground Truths

(c) Pix2Pix segmentation images

Fig.3. The samples of test images, there related ground truths and their experimental results

3.5 Evaluation to the most advanced technique, U-Net

The algorithm for comparison was U-Net. We equated the Pix2Pix with the U-Neton ILD data set. 41 samples from the test set were tested, while 67 samples from the training set were used for training. The accuracy, the overlap rate andthe F measure with standard deviation of the two algorithms were compared. Additionally, we compared the training and testing times for the two approaches. Table 2 displays the outcomes of the comparison. Pix2Pix has greater segmentation accuracy, F measure and overlap rate when compared to U-Net. The comparison findings demonstrate Pix2Pix's superior segmentation capability. Be aware that the performance of Pix2Pix was far from optimal when 67 samples were used for training. The Pix2Pix algorithm required half as much time to train and test as U-Net, proving that it is more time-effective.

Table 2. Outcomes of the evaluation among Pix2Pix and U-Net

	accuracy	overlap rate	F measure	training time	test time
U-Net	0.821 ±0.070	0.691 ±0.110	0.812 ±0.085	12 hours	6min12s
Pix2Pix	0.834 ±0.082	0.785 ±0.156	0.870 ±0.114	6 hours	2min23s

4. Conclusion

Present study suggested a Pix2Pix-based Lung segmentation technique. The segmented image was created by translating the unique lung image with the Pix2Pix. On a real lung imaging data set, the Pix2Pix segmentation approach was evaluated. The projected method is effective and outdoesadvanced methods, according to experimental results.

• Conflict of interest disclosure- The authors declare that they have no known competing financial interests or personal relationships that could have appeared to influence the work reported in this paper.

REFERENCES

1. R. Shah, S. Sabanathan, J. Richardson, A. Mearns, C. Goulden, Results of surgical treatment of stage i and ii lung cancer., J. Cardiovasc. Surg. 37 (1996) 169–172.
2. J.C. Nesbitt, J.B. Putnam Jr., G.L. Walsh, J.A. Roth, C.F. Mountain, Survival in early-stage non-small cell lung cancer, Ann. Thorac. Surg. 60 (1995) 466–472.
3. W.R. Webb, N.L. Muller, D.P. Naidich, High-Resolution CT of the Lung, LippincottWilliams & Wilkins, (2014).
4. Depeursinge, A. Vargas, A. Platon, A. Geissbuhler, P.-A. Poletti, H. Müller,Building a reference multimedia database for interstitial lung diseases, Comput.Med. Imaging Graph.36 (2012) 227–238.
5. J. Pu, J. Roos, A.Y. Chin, S. Napel, G.D. Rubin, D.S. Paik, Adaptive bordermarching algorithm: automatic lung segmentation on chest ct images, Comput.Med. Imaging Graph.32 (2008) 452–462.
6. G. Singadkar, A. Mahajan, M. Thakur, S. Talbar, Automatic lung segmentation for the inclusion of juxtapleural nodules and pulmonary vessels using curvaturebased border correction, J. King Saud Univ.-Comput. Inf. Sci. (2018).
7. E.M. van Rikxoort, B. de Hoop, M.A. Viergever, M. Prokop, B. van Ginneken, Automatic lung segmentation from thoracic computed tomography scans usinga hybrid approach with error detection, Med. Phys. 36 (2009) 2934–2947.
8. M.S. Brown, J.G. Goldin, M.F. McNitt-Gray, L.E. Greaser, A. Sapra, K.-T. Li,J.W. Sayre, K. Martin, D.R. Aberle, Knowledge-based segmentation of thoracic computed tomography images for assessment of split lung function, Med. Phys.27 (2000) 592–598.
9. M.S. Brown, M.F. Mcnitt-Gray, N.J. Mankovich, J.G. Goldin, J. Hiller, L.S. Wilson,D. Aberie, Method for segmenting chest ct image data using an anatomical model: preliminary results, IEEE Trans. Med. Imaging 16 (1997) 828–839.
10. X. Sun, H. Zhang, H. Duan, 3d computerized segmentation of lung volume with computed tomography, Acad. Radiol. 13 (2006) 670–677.
11. S. Hu, E.A. Hoffman, J.M. Reinhardt, Automatic lung segmentation for accurate quantitation of volumetric x-ray ct images, IEEE Trans. Med. Imaging 20 (2001)490–498.
12. J.K. Leader, B. Zheng, R.M. Rogers, F.C. Sciurba, A. Perez, B.E. Chapman, S.Patel, C.R. Fuhrman, D. Gur, Automated lung segmentation in x-ray computedtomography: development and evaluation of a heuristic threshold-based scheme1,Acad. Radiol. 10 (2003) 1224–1236.
13. S.G. Armato III, W.F. Sensakovic, Automated lung segmentation for thoracic ct:Impact on computer-aided diagnosis1, Acad. Radiol. 11 (2004) 1011–1021.
14. Sluimer, M. Prokop, B. Van Ginneken, Toward automated segmentation of the pathological lung in ct, IEEE Trans. Med. Imaging 24 (2005) 1025–1038.
15. M.N. Prasad, M.S. Brown, S. Ahmad, F. Abtin, J. Allen, I. da Costa, H.J. Kim,M.F. McNitt-Gray, J.G. Goldin, Automatic segmentation of lung parenchyma inthe presence of diseases based on curvature of ribs, Acad. Radiol. 15 (2008)1173–1180.
16. E.E. Nithila, S. Kumar, Segmentation of lung from ct using various active contourmodels, Biomed. Signal Process. Control 47 (2019) 57–62.
17. Q. Abbas, Segmentation of differential structures on computed tomographyimages for diagnosis lung-related diseases, Biomed. Signal Process. Control 33(2017) 325–334.
18. S. Zhou, Y. Cheng, S. Tamura, Automated lung segmentation and smoothingtechniques for inclusion of juxtapleural nodules and pulmonary vessels on chestct images, Biomed. Signal Process. Control 13 (2014) 62–70.
19. Y. Iwao, T. Gotoh, S. Kagei, T. Iwasawa, M. de Sales Guerra Tsuzuki, Integratedlung field segmentation of injured region with anatomical structure analysis byfailure–recovery algorithm from chest ct images, Biomed. Signal Process. Control12 (2014) 28–38, Model
20. Based Image and Signal Processing Methods for BetterMedical Treatment. X. Ye*, X. Lin, J. Dehmeshki, G. Slabaugh, G. Beddoe, Shape-based computeraided detection of lung nodules in thoracic ct images, IEEE Trans. Biomed. Eng.56 (2009) 1810–1820.
21. W.-J. Choi, T.-S. Choi, Genetic programming-based feature transform andclassification for the automatic detection of pulmonary nodules on computedtomography images, Inform. Sci. 212 (2012) 57–78.
22. S. Shen, A.A. Bui, J. Cong, W. Hsu, An automated lung segmentation approachusing bidirectional chain codes to improve nodule detection accuracy, Comput.Biol. Med. 57 (2015) 139–149.
23. P. Swierczynski, B.W. Papież, J.A. Schnabel, C. Macdonald, A level-set approachto joint image segmentation and registration with application to ct lung imaging,Comput. Med.Imaging Graph. 65 (2018) 58–68, Advances in Biomedical ImageProcessing.
24. A.A. Farag, H.E.A.E. Munim, J.H. Graham, A.A. Farag, A novel approach for lungnodules segmentation in chest ct using level sets, IEEE Trans. Image Process. 22(2013) 5202–5213.
25. W. Zhang, X. Wang, P. Zhang, J. Chen, Global optimal hybrid geometric activecontour for automated lung segmentation on ct images, Comput. Biol. Med. 91(2017) 168–180.
26. P.P.R. Filho, P.C. Cortez, A.C. da Silva Barros, V.H.C. Albuquerque, J.M.R.S.Tavares, Novel and powerful 3d adaptive crisp active contour method appliedin the segmentation of ct lung images, Med. Image Anal. 35 (2017) 503–516.
27. E. Hosseini-Asl, J.M. Zurada, G. Gimel'farb, A. El-Baz, 3-d lung segmentation by incremental constrained nonnegative matrix factorization, IEEE Trans. Biomed.Eng. 63 (2015) 952–963.
28. E. Hosseini-Asl, J.M. Zurada, A. El-Baz, Lung segmentation based on nonnegativematrix factorization, in: 2014 IEEE International Conference on Image Processing(ICIP), IEEE, 2014, pp. 877–881.
29. S. Wang, M. Zhou, Z. Liu, Z. Liu, D. Gu, Y. Zang, D. Dong, O. Gevaert, J. Tian,Central focused convolutional neural networks: Developing a data-driven modelfor lung nodule segmentation, Med. Image Anal. 40 (2017) 172–183.
30. A.A.A. Setio, F. Ciompi, G. Litjens, P. Gerke, C. Jacobs, S.J. Van Riel, M.M.W.Wille, M. Naqibullah, C.I. Sánchez, B. van Ginneken, Pulmonary nodule detectionin ct images: false positive reduction using multi-view convolutional networks,IEEE Trans. Med. Imaging 35 (2016) 1160–1169.
31. G. Tong, Y. Li, H. Chen, Q. Zhang, H. Jiang, Improved u-net network forpulmonary nodules segmentation, Optik 174 (2018) 460–469.
32. T. Lan, Y. Li, J.K. Murugi, Y. Ding, Z. Qin, Run: Residual u-net for computeraided detection of pulmonary nodules without candidate selection, 2018, ArXivabs/1805.11856.
33. M.Z. Alom, M. Hasan, C. Yakopcic, T.M. Taha, V.K. Asari, Recurrent residual convolutional neural network based on u-net (r2u-net) for medical imagesegmentation, 2018, ArXiv abs/1802.06955.
34. Y. Gu, X. Lu, L. Yang, B. Zhang, D. Yu, Y. Zhao, L. Gao, L. Wu, T. Zhou,Automatic lung nodule detection using a 3d deep convolutional neural networkcombined with a multi-scale prediction strategy in chest cts, Comput. Biol. Med.103 (2018) 220–231.
35. A.P. Harrison, Z. Xu, K. George, L. Lu, R.M. Summers, D.J. Mollura, Progressive and multi-path holistically nested neural networks for pathological lungsegmentation from ct images, in: MICCAI, 2017.
36. X. Liu, S. Guo, B. Yang, S. Ma, H. Zhang, J. Li, C. Sun, L. Jin, X. Li, Q.Yang, Y. Fu, Automatic organ segmentation for ct scans based on super-pixeland convolutional neural networks, J. Digit. Imaging 31 (2018) 748–760.
37. M. Xu, S. Qi, Y. Yue, Y. Teng, L. Xu, Y. Yao, W. Qian, Segmentation oflung parenchyma inct images using cnn trained with the clustering algorithmgenerated dataset, in: Biomedical engineering online, 2019.
38. M. Negahdar, D. Beymer, T.F. Syeda-Mahmood, Automated volumetric lungsegmentation of thoracic ct images using fully convolutional neural

network,in: Medical Imaging, 2018.
39. H.R. Roth, L. Lu, N. Lay, A.P. Harrison, A. Farag, A. Sohn, R.M. Summers, Spatial aggregation of holistically-nested convolutional neural networks for automatedpancreas localization and segmentation, Med. Image Anal. 45 (2018) 94–107.
40. C. Liu, M. Pang, Automatic lung segmentation based on image decompositionand wavelet transform, Biomed. Signal Process. Control 61 (2020) 102032.
41. D.D. Lee, H.S. Seung, Learning the parts of objects by non-negative matrix factorization, Nature 401 (1999) 788–791.
42. P. Patil, S. Murala, Fggan: A cascaded unpaired learning for backgroundestimation and foreground segmentation, in: 2019 IEEE Winter Conference onApplications of Computer Vision (WACV), IEEE, 2019, pp. 1770–1778.
43. P.W. Patil, O. Thawakar, A. Dudhane, S. Murala, Motion saliency based generative adversarial network for underwater moving object segmentation, in:2019 IEEE International Conference on Image Processing (ICIP), IEEE, 2019, pp.1565–1569.
44. P. Hambarde, S.N. Talbar, N. Sable, A. Mahajan, S.S. Chavan, M. Thakur,Radiomics for peripheral zone and intra-prostatic urethra segmentation in mrimaging, Biomed. Signal Process. Control 51 (2019) 19–29.
45. Dudhane, S. Murala, Ryf-net: Deep fusion network for single image haze removal, IEEE Trans. Image Process. 29 (2019) 628–640.
46. K. Simonyan, A. Zisserman, Very deep convolutional networks for large-scale image recognition, 2014, arXiv preprint arXiv:1409.1556.
47. C. Szegedy, W. Liu, Y. Jia, P. Sermanet, S. Reed, D. Anguelov, D. Erhan, V.Vanhoucke, Rabinovich, Going deeper with convolutions, in: Proceedings ofthe IEEE Conference on Computer Vision and Pattern Recognition, 2015, pp.1–9.
48. G. Huang, Z. Liu, L. Van Der Maaten, K.Q. Weinberger, Densely connected convolutional networks, in: Proceedings of the IEEE Conference on ComputerVision and Pattern Recognition, 2017, pp. 4700–4708.
49. K. He, X. Zhang, S. Ren, J. Sun, Deep residual learning for image recognition, in: Proceedings of the IEEE Conference on Computer Vision and Pattern Recognition, 2016, pp. 770–778.
50. S. Nema, A. Dudhane, S. Murala, S. Naidu, Rescuenet: An unpaired gan for braintumor segmentation, Biomed. Signal Process. Control 55 (2020) 101641.
51. G. Singadkar, A. Mahajan, M. Thakur, S. Talbar, Deep deconvolutional residual network based automatic lung nodule segmentation, J. Digit. Imaging 33 (2020)678–684.
52. F. Milletari, N. Navab, S.-A. Ahmadi, V-net: Fully convolutional neural networks for volumetric medical image segmentation, in: 2016 Fourth InternationalConference on 3D Vision (3DV), IEEE, 2016, pp. 565–571.
53. P. Isola, J.-Y. Zhu, T. Zhou, A.A. Efros, Image-to-image translation with conditional adversarial networks, in: 2017 IEEE Conference on Computer Vision and Pattern Recognition (CVPR), IEEE, 2017, pp. 5967–5976.
54. Y. Song, W. Cai, Y. Zhou, D.D. Feng, Feature-based image patch approximationfor lung tissue classification, IEEE Trans. Med. Imaging 32 (2013) 797–808.
55. D. Ulyanov, A. Vedaldi, V. Lempitsky, Instance normalization: The missingingredient for fast stylization, 2016, arXiv preprint arXiv:1607.08022.
56. O. Ronneberger, P. Fischer, T. Brox, U-net: Convolutional networks forbiomedical image segmentation, in: International Conference on Medical ImageComputing and Computer-Assisted Intervention, Springer, 2015, pp. 234–241.
57. A.G. Howard, M. Zhu, B. Chen, D. Kalenichenko, W. Wang, T. Weyand, M.Andreetto, H. Adam, Mobilenets: Efficient convolutional neural networks formobile vision applications, 2017, arXiv preprint arXiv:1704.04861.
58. R.L. Siegel, K.D. Miller, A. Jemal, Cancer statistics, CA Cancer J. Clin. 70 (2020) 7–30.
59. Khairandish, Mohammad Omid, R. Gurta, and Meenakshi Sharma. "A hybrid model of faster R-CNN and SVM for tumor detection and classification of MRI brain images." Int. J. Mech. Prod. Eng. Res. Dev 10.3 (2020): 6863-6876.
60. Ranjith, C., C. Hemamalini, and K. Senthil Kumar. "An Analysis of the Health Hazards of Workers in Transport Industry." International Journal of Business Management & Research (IJBMR) 7.2: 9-16.
61. Moffatt, Stanley, and Mutune Wangari. "Enhanced Silencing of Bmi-1 and Htert Gene Expression with Ngr-Pei-Coupled Sirna Lipoprotein Nano-Complexes." TJPRC: Journal of Medicine and Pharmaceutical Science (TJPRC: JMPS) 2 (2016): 9-18.
62. Kodali, Swetha, and A. Mrunalini. "Occupational Health Problems among Workers in Concrete Based Manufacturing Industry–A Review of Research." International Journal of Educational Science and Research (IJESR) 8.4: 39-44.
63. Sheeba, A., A. Sangaran, and B. R. Latha. "Hydatid Cyst In Liver-A Case Report in Human." International Journal of Medicine and Pharmaceutical Sciences (IJMPS) 5.2 (2015): 59-62.